

Arginine decarboxylase expression, polyamines biosynthesis and reactive oxygen species during organogenic nodule formation in hop

Ana M. Fortes,^{1,†,*} Joana Costa,^{1,†} Filipa Santos,² José M. Seguí-Simarro,³ Klaus Palme,^{2,5} Teresa Altabella,⁴ Antonio F. Tiburcio⁴ and Maria S. Pais¹

¹Plant Systems Biology Lab; Center for Biodiversity, Functional and Integrative Genomics (BioFIG); ICAT; FCUL; Lisboa, Portugal; ²Institute for Biology II/Botany; Faculty of Biology; University of Freiburg; Germany; ³Instituto para la Conservación y Mejora de la Agrodiversidad Valenciana (COMAV) - Universitat Politècnica de València, Valencia, Spain; ⁴Unitat de Fisiologia Vegetal; Facultat de Farmàcia; Universitat de Barcelona; Barcelona, Spain; ⁵Freiburg Institute of Advanced Studies (FRIAS); Albert-Ludwig's University; Freiburg, Germany

[†]These authors contributed equally to this paper.

Key words: arginine decarboxylase, *Humulus lupulus*, morphogenesis, organogenic nodule, polyamines, reactive oxygen species

Abbreviations: ADC, arginine decarboxylase; DAB, diaminobenzidine; DAO, diamine oxidase; NBT, nitroblue tetrazolium; ODC, ornithine decarboxylase; PAO, polyamine oxidase; PAs, polyamines; ROS, reactive oxygen species; SAMDC, *S*-adenosyl-L-methionine decarboxylase; SPDS, spermidine synthase; SPMS, spermine synthase

Hop (*Humulus lupulus* L.) is an economically important plant species used in beer production and as a health-promoting medicine. Hop internodes develop upon stress treatments organogenic nodules which can be used for genetic transformation and micropropagation.

Polyamines are involved in plant development and stress responses. Arginine decarboxylase (ADC; EC 4.1.1.19) is a key enzyme involved in the biosynthesis of putrescine in plants. Here we show that ADC protein was increasingly expressed at early stages of hop internode culture (12 h). Protein continued accumulating until organogenic nodule formation after 28 days, decreasing thereafter. The same profile was observed for ADC transcript suggesting transcriptional regulation of ADC gene expression during morphogenesis. The highest transcript and protein levels observed after 28 days of culture were accompanied by a peak in putrescine levels. Reactive oxygen species accumulate in nodular tissues probably due to stress inherent to in vitro conditions and enhanced polyamine catabolism. Conjugated polyamines increased during plantlet regeneration from nodules suggesting their involvement in plantlet formation and/or in the control of free polyamine levels.

Immunogold labeling revealed that ADC is located in plastids, nucleus and cytoplasm of nodular cells. In vacuolated cells, ADC immunolabelling in plastids doubled the signal of proplastids in meristematic cells. Location of ADC in different subcellular compartments may indicate its role in metabolic pathways taking place in these compartments.

Altogether these data suggest that polyamines play an important role in organogenic nodule formation and represent a progress towards understanding the role played by these growth regulators in plant morphogenesis.

Introduction

Polyamines are ubiquitous low molecular weight aliphatic amines that occur in living organisms either as free cations or conjugates bound to phenolic acids and polyanionic macromolecules such as proteins and nucleic acids.¹ They have been implicated in a wide range of biological processes, including cell growth and division, stabilization of nucleic acids and membranes, protein synthesis and chromatin function, and biotic and abiotic stresses responses.²⁻⁵

The most common PAs are spermidine and spermine, together with their diamine precursor putrescine. The biosynthesis of PAs is controlled in plants primarily by three enzymes: arginine decarboxylase (ADC; EC 4.1.1.19) and ornithine decarboxylase (ODC;

EC 4.1.1.17), which are responsible for the production of putrescine and *S*-adenosyl-L-methionine decarboxylase (SAMDC; EC 4.1.1.50), which is necessary for the synthesis of spermidine and spermine. The enzymes spermidine and spermine synthases (SPDS; EC: EC 2.5.1.16; SPMS; EC 2.5.1.16) are also involved in the synthesis of the triamine and tetraamine, respectively. The intracellular free PA pool is affected both by PA synthesis and degradation, and by mechanisms of cellular influx, efflux and conjugation.¹ Polyamines are catabolized mostly by diamine and polyamine oxidases.⁶ Diamine oxidase (DAO, EC 1.4.3.6) catabolizes putrescine to form pyrroline, hydrogen peroxide and ammonia, whereas polyamine oxidase (PAO, EC 1.5.3.3) oxidizes spermidine or spermine forming pyrroline, diamine propane and

*Correspondence to: Ana Margarida Fortes; Email: amfortes@fc.ul.pt
Submitted: 11/22/10; Revised: 12/10/10; Accepted: 12/16/10
DOI: 10.4161/psb.6.2.14503

hydrogen peroxide or diazabicyclononane, diamine propane and hydrogen peroxide, respectively.⁶ Plant amine oxidases regulate cellular levels of PAs and contribute to important physiological processes through their reaction products.⁶ In particular, 4-aminobutanal can be further metabolized to γ -aminobutyric acid (GABA), a non-protein amino acid that can be also produced by cytosolic glutamate decarboxylase.⁶

The relative proportions of free and conjugated PAs varied from species to species. Compared to the intensive attention which has been focused on changes in free PAs in response to stress, alteration of the conjugated form has been less well characterized although stress-induced accumulation of conjugated PAs has been reported in reference 7 and 8. Large levels of conjugated putrescine at an early stage of salt stress accumulate in apple.⁷

Mammalian and fungal cells utilize mainly ODC to synthesize putrescine. It has been postulated that plants have acquired the ability to produce putrescine via ADC to meet specific requirements during normal development and also during adaptation to environment⁹ such as in response to stress and in wound or hormone response. Putrescine is generally known to increase under many stress conditions.^{9,10} The involvement of PAs in stress response is well established for several plant species, although their precise role is still unclear.² Spermidine and spermine present anti-senescent properties,¹¹ and yet, they may inhibit growth and induce oxidative stress; these PAs increased nitric oxide release in *Arabidopsis thaliana* seedlings.¹² Polyamines have been related to apoptosis and programmed cell death.¹³ Recently, PA catabolism resulting in hydrogen peroxide accumulation was shown to preinduce tolerance of tobacco against pathogens and PA homeostasis was maintained by induction of the arginine decarboxylase pathway.¹⁴ The manipulation of the PA biosynthetic pathway, through overexpression of various genes involved in PA biosynthesis confers increased tolerance to several abiotic stresses.² Exposure of plant cells to stress is associated with oxidative damage at cellular level. The reactive oxygen species (ROS), including H_2O_2 , are responsible for the oxidative stress. It is known that PAs are capable of protecting membranes against ROS-induced lipid peroxidation.¹⁵ Moreover, PAs inhibit NADPH oxidase-mediated superoxides generation.¹⁶

Somatic embryogenesis and organogenic nodule formation are important morphogenic processes. Nodular structures have been studied in several plant species and were found to be an additional morphogenic pathway useful for regeneration strategies, automated micropropagation and genetic transformation for desirable characteristics.¹⁷ The lack of efficient regeneration protocols for some agricultural plants and trees is a major limitation for their improvement through genetic engineering. Hop, besides being an important ingredient in beer, has very promising health-promoting and medicinal properties given mainly by specific polyphenols.^{18,19} In spite of its economical importance, hop is extremely sensitive to several pathogens. Therefore, it is important to continue research towards understanding factors involved on in vitro plant regeneration. Organogenic nodule formation is a morphogenic process that shares features with somatic embryogenesis though in the former no shoot/root pole is established and plantlet regeneration can occur from different peripheral regions

of nodules.²⁰ Organogenic nodule formation and the involvement of wounding in their induction have been previously described in hop (*Humulus lupulus* L.).^{21,22}

Recent studies carried out during morphogenesis in hop showed increased transcription in prenodules and nodules of genes coding for SAM synthetase, SAMDC and a cobalamine-independent methionine synthase suggesting increased SAM, spermidine and spermine synthesis.²³ Stress related compounds such as GABA, glutamine and glutathione accumulated throughout hop culture in particular during nodule formation whereas arginine presented an opposite trend.²³

In this study, we aim at complementing the information already gathered related to involvement of oxidative stress and growth regulators in organogenic nodule formation. The present data suggests a link between ADC expression, PAs biosynthesis and organogenic nodule formation.

Results

ADC accumulation throughout organogenic nodule formation. Protein gel blot analysis was carried out to evaluate ADC expression and accumulation during induction and formation of organogenic nodules. At the time of internodes inoculation two bands with a molecular mass of approximately 24 kD and 54 kD corresponding to ADC protein were detected. The 54 kD band kept approximately constant throughout the different morphogenic stages, except for the stage of prenodule when a considerable increase in its levels was noticed. During the first week, when divisions are occurring in cambial and cortical cells of internodes,²⁰ ADC protein level constantly increased mainly due to an increase in the 24 kD protein polypeptide. In nodules which appear 28 days upon internode inoculation, this ADC polypeptide reached its highest level, then dropping to non detectable levels at about 45 days of culture (Fig. 1), during which plantlet regeneration occurs from nodules. The 54 kD band also decreased at this morphogenic stage, though to a lower extent than the 24 kD band (Fig. 1).

Subcellular localization of ADC in plastids, cytoplasm and nucleus. The subcellular localization of the ADC protein in different cell types was analyzed by immunogold labeling at three time points during organogenic nodule formation: 7 days of culture (Fig. 2), 28 days of culture corresponding to nodules formation (Figs. 3 and 4) and 45 days of culture corresponding to plantlet regeneration (data not shown). Seven days upon wounding cell divisions are occurring in cambial and cortical cells (Fig. 2A and B). Cortical cells were surrounded by degenerating cells, probably undergoing cell death (Fig. 2B arrow). Gold particles appeared over the nucleus, cytoplasm and plastids of cortical cells but not in vacuoles and Golgi stacks (Fig. 2C). Immunogold labeling also appeared in the nucleus and cytoplasm of both meristematic (Fig. 3A–C) and differentiated nodular cells (Fig. 4A–C). Gold particles appeared dispersed throughout the cytoplasm as well as in plastids (Figs. 3C and 4A and B). In the nucleus, signal was found dispersed at the interchromatin region and sometimes at the borders of condensed chromatin masses (Fig. 4A). As long as the ultrastructure of plastid membranes

can be discerned in Lowicryl-embedded samples, gold particles were never found on grana, labeling being restricted to the stroma (Fig. 4B). Signal was rarely or not found over other cytoplasmic organelles as vacuoles or cell wall (Fig. 4A and B). Controls excluding the anti-ADC antibody or substituting it by preimmune serum did not show significant labelling over any subcellular region (Fig. 4C).

In order to obtain detailed information regarding the different subcellular distribution of ADC in proliferative versus highly vacuolated nodular cells (Figs. 3 and 4), immunogold labeling was quantified in both cell types. Unspecific background signal was also quantified over the cell walls, vacuoles, starch deposits and resin present in the micrographs. Data showed that it never exceeded 5% of the estimated signal. For both proliferating and differentiated cells (Fig. 5), immunogold particles were twice more abundant in cytoplasm than in nucleus, being the mean labeling density not statistically different ($\alpha \leq 0.05$) between both cell types (0.7 ± 0.30 particles/cytoplasmic μm^2 and 0.3 ± 0.24 particles/nuclear μm^2 in proliferating cells and 0.8 ± 0.38 particles/cytoplasmic μm^2 and 0.4 ± 0.21 particles/nuclear μm^2 in vacuolated cells). However, the mean labeling density was significantly different in the case of plastids, where almost twice the mean labeling density was found in plastids of vacuolated cells versus those of proliferating cells (1.2 ± 0.65 and 0.7 ± 0.28 particles/ μm^2 , respectively), suggesting that in differentiated cells ADC accumulates in plastids.

ADC transcript accumulation during morphogenic stages. To test whether the observed ADC protein accumulation was due to increased ADC mRNA, a cDNA fragment of 1,663 bp was cloned presenting 80% identity to *Cucumis sativus* arginine decarboxylase (ADC) (GenBank Acc. AY274822) at the protein level. Expression of hop ADC (GenBank Acc. Q981435) was analyzed for most informative time points (T0, T15d, T28d, T45d) using qRT-PCR. During morphogenesis in particular during prenodule and nodule formation (T28d) a significant increase in ADC mRNA accumulation was found followed by a decrease at T45d (Fig. 6).

Increase in polyamines during nodule formation. During organogenic nodule induction, all three PAs were present both in free and conjugated forms (Fig. 7A–C). The most abundant PA throughout the process was putrescine either in free or conjugated forms. The exception was for the TCA-insoluble fraction (Fig. 7C) in which spermidine was found in a higher concentration at days 28 and 45 (1.6- and 1.9-fold higher, respectively). Spermine presented the lowest concentration in all three fractions quantified (free, TCA-soluble and TCA-insoluble conjugated). In all three forms putrescine content started to increase from day 4, reaching the highest measured values at day 28 and declining at day 45. Spermidine and spermine showed a similar profile though the increase in these PAs was more moderate up to day 15. The time-course analysis of the contents of

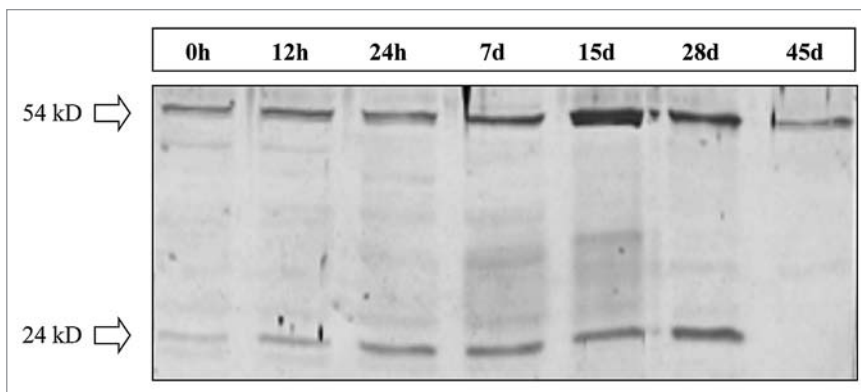


Figure 1. Immunoblot analysis of ADC. Protein extracts corresponding to several culture stages are represented (0, 12 and 24 hours, and 7, 15, 28 and 45 days). 30 μg total protein extract was loaded per lane.

all three PAs (putrescine, spermidine and spermine) showed a similar trend in the different fractions being the TCA-insoluble conjugates detected only in small amounts comparing to both free and soluble conjugated PAs (Fig. 7C). Changes in the ratio between free and conjugated forms during organogenic nodule formation are shown in Figure 8. At day 15 the level of free PAs was 1.55-fold higher comparing to the conjugated forms. From day 28 onwards there was a marked enhancement in the level of conjugated PAs, with a shift on the ratio between conjugated and free forms from 0.7 at day 15 to 1.62 at day 28 and 1.92 at day 45. This shift was mainly due to soluble and insoluble conjugated forms of spermidine (Fig. 7B and C). Interestingly, though the amounts of soluble conjugates of spermidine are much higher than insoluble conjugates of spermidine after 28 days (960.99 nmolmgprotein⁻¹ and 118.02 nmolmgprotein⁻¹, respectively), the insoluble conjugates showed an higher increase in between days 15 and 28 (27.0-fold comparing to 18.2-fold). During the period of 15 and 28 days total free PAs increased 5.2-fold whereas total soluble and insoluble conjugates increased 9.3- and 10.7-fold, respectively.

In situ staining of reactive oxygen species. Immediately after excision of internodes from the parental plant, ROS production could be observed scattered throughout the internode (Fig. 9A). Twenty-four hours after internodes inoculation, increase in ROS was detected mainly in areas previously submitted to wounding as shown by NBT treatment (Fig. 9B arrow). The in situ detection of hydrogen peroxide, as early as 12 h after culture initiation, showed a strong DAB staining restricted to the wounded areas (not shown). After 7 days in solid medium, the explants started forming calli in the previously wounded regions.²⁰ These structures appeared dark purple after NBT treatment (Fig. 9C arrow). After 15 days in culture, NBT staining was observed mainly in calli cells and in prenodular structures (Fig. 9D and E). Additionally, diaminobenzidine staining showed that hydrogen peroxide accumulation intensified from the inner to the outer layers of prenodules (Fig. 9F). During nodule development ROS production could be observed in regions of future nodule separation (Fig. 9G black arrow) and in calli tissues formed due to proliferation of explant cells and that surround nodular clusters

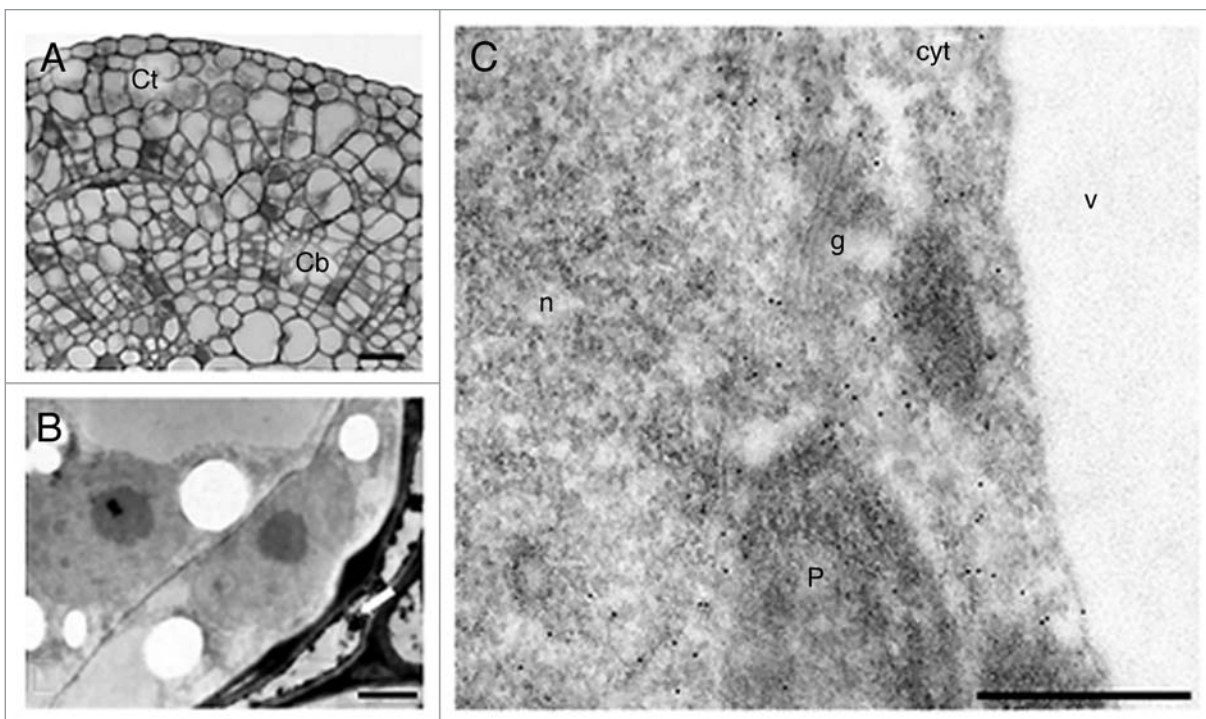


Figure 2. Anti-ADC immunogold labeling in hop internodes after seven days of culture. (A) Semi-thin section showing divisions in cortical (Ct) and cambial cells (Cb). (B) Ultra-thin section showing cortical cells undergoing division and surrounded by cells undergoing cell death (arrow). (C) Ultra-thin section showing labeling in the cytoplasm (cyt), nucleus (n) and plastids (p). Labeling is absent in vacuoles (v) and golgi vesicles (g). Bars: A = 100 μm ; B = 2.5 μm ; C = 500 nm.

(Fig. 9G white arrow). Nodule separation appears to be initiated by the formation of a necrotic layer at the region of future nodule separation which accumulates reactive oxygen species.²¹

Discussion

Polyamines are involved in developmental processes, including cell growth and morphogenesis.^{2,3} In *in vitro* cultures of hop internodes, we describe a high increase in total PAs content four days after culture initiation, probably related to the onset of active cambial and cortical cell division. Polyamine synthesis, abundance and distribution seem to correlate positively with cell division.²⁴ They have long been recognized as cell proliferation and differentiation regulators.²⁵ Totipotent-tobacco protoplasts, with high division rates, have the highest level of endogenous PAs.²⁶ Total putrescine predominates over spermidine and spermine during organogenic nodule induction and formation in hop. This is in accordance with the results obtained in tobacco for totipotent-protoplasts.²⁶ Recalcitrant-grapevine protoplasts showed a lower PA content and a higher ratio of spermine to total PAs which suggests that the levels and metabolism of the intracellular PAs could be related to the expression of totipotency of plant protoplasts.²⁶ It may be that PAs play a role in the expression of determination for organogenic nodule formation in hop. Polyamines content kept increasing up to nodule formation reaching huge values at this time point.

Polyamines are also known to enhance extracellular signal regulated kinase (ERK) activity²⁷ playing a role in signal

transduction events leading to cell growth and differentiation. The differential expression, activation and localization of two extracellular signal regulated kinase isoforms has been reported for hop morphogenesis.²² One of these isoforms (ERK1) was specifically involved in stages when separation of nodules into daughter nodules and meristem formation occur (28 and 45 days after induction). Polyamines have also been related to other morphogenic processes such as somatic and zygotic embryogenesis.^{3,28-30} In embryogenic regions of *Camellia* leaves, time course analysis of PAs content suggested that soluble and insoluble conjugated putrescine and soluble conjugated spermidine are related to the formation and development of globular embryos.²⁹ Polyamines were suggested to be involved in polar auxin transport, in the differentiation of vascular tissues and in the definition of vein positions.³¹ It may be that the huge amount of PAs detected in hop nodules 28 days after culture initiation are also related to differential auxin fluxes inside nodules which may lead to organization of nodular vascular centers to which future regenerated plantlets will be connected to.^{19,20} It is noteworthy in this context that hop nodules contain higher levels of IAA than internodes.³²

In Scots pine, at the early developmental stages of zygotic embryogenesis there is typically an increasing trend in PA concentrations and a decreasing trend during late embryo development.³ This is also observed during organogenic nodule formation. When shoot buds have been formed and plantlet regeneration starts there is a significant drop in PAs content which may be

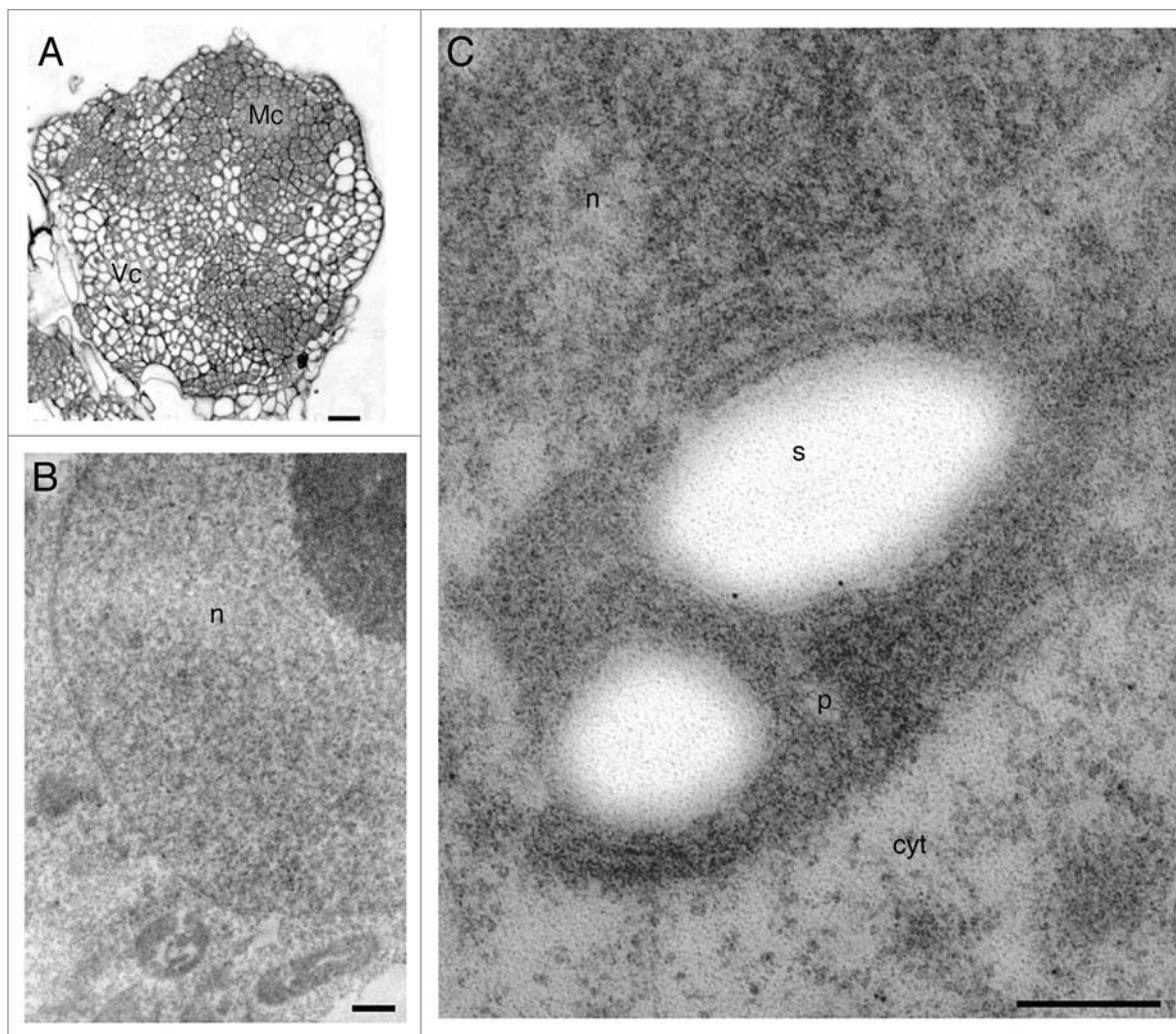


Figure 3. Anti-ADC immunogold labeling in meristematic nodular cells after 28 days of culture. (A) Semi-thin section showing meristematic (Mc) and vacuolated cells (Vc) of nodules. (B) Magnification of meristematic cells. (C) Meristematic cell showing gold particles over nucleus, cytoplasm and plastids. Bars: A = 100 μ m; B = 400 nm; C = 300 nm.

related to the expression of morphogenic capacity of the tissue in culture and protection against oxidative stress.

In protein extracts of hop internodes and nodules the anti-ADC antibody from tobacco detected two bands with approximate molecular masses of 54 and 24 kD. In protein extracts of tobacco leaves, the anti-ADC antibodies detected a band with approximate molecular mass of 77 kD, and a smaller band of 54 kD. The 54 kD protein may be an ADC form present only in the chloroplast of photosynthetic tissues.³³ The recognition in hop extracts of a band of a molecular mass of 24 kD using a tobacco polyclonal antibody is not surprising since it has been reported for other plant species such as oat,³⁴ where ADC is synthesized as a pre-protein of 66 kD, which is cleaved to produce a fragment of 42 kD (containing the original amino terminus) and a 24 kD polypeptide (containing the original carboxyl terminus), these two processed polypeptides being held together by disulfide bonds.³⁵

During organogenic nodule formation in hop, depending on the tissue, ADC is located in three different compartments:

nucleus, plastids and cytosol. ADC activity has been localized mainly in the chloroplast of photosynthetic tissues and in the nucleus of the non-photosynthetic tissues.³³ The subcellular localization of ODC and ADC indicate that both proteins are also active in cytosolic fraction.²⁴ This differential subcellular localization observed in plant cells was also shown for ODC in animal tissues and may be cell type-specific and/or dependent on the physiological status.³⁶

ADC can play different roles depending on its subcellular localization.³³ Its presence in chloroplast may be related to photosynthesis. A correlation among PA concentration, chlorophyll biosynthesis and photosynthetic rate has been demonstrated.³⁷ In organogenic nodules differentiated cells containing chloroplasts present more ADC in this cellular compartment than proliferating cells in plastids, suggesting that in those cells PAs may be related to photosynthesis. Studies in mammalian cells showed direct binding of PAs to nucleic acids and ability to modulate their conformation and interaction with proteins, playing a role in cellular signaling.⁴ At different phases of mitosis in Scots pine

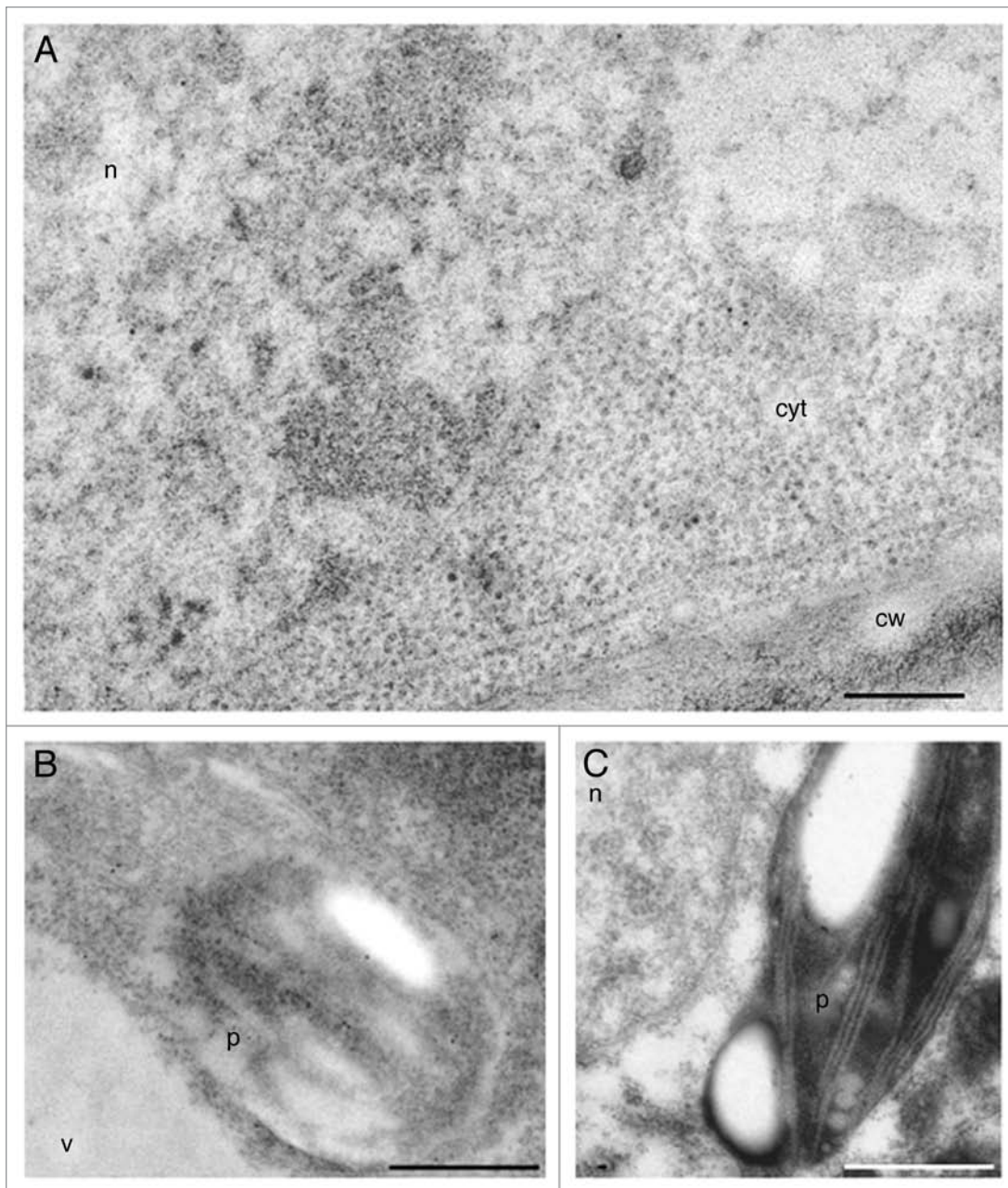


Figure 4. Anti-ADC immunogold labeling in differentiated nodular cells after 28 days of culture. (A and B) Differentiated cells, highly vacuolated showing significant labeling in the cytoplasm, nucleus and plastids. No labeling is observed in cell wall (cw) and vacuoles (v). (C) Control of immunogold labeling with preimmune anti-ADC. Bar in A = 250 nm. Bars in B and C = 1 μ m.

zygotic embryogenesis *ADC* mRNA, and ADC protein is localized in dividing cells of embryo meristems and more specifically within the mitotic spindle apparatus and close to the chromosomes, respectively. It may be that ADC presence in nucleus of hop cells as reported here may play a role in mitosis and signaling events.³

The involvement of transcriptional regulation in the expression of ADC has been suggested since during morphogenesis in Scots pine both ADC gene expression and ADC protein synthesis increased.³ On the other hand, ADC has been reported to be regulated at the posttranslational level.³⁴ This indicates that different

regulation mechanisms may be involved in ADC expression in different gene family members, plant species, tissues and physiological conditions, as well as at different developmental stages.

Since our results point to a transcriptional regulation of ADC during organogenic nodule formation as it was found during embryogenesis in pine³ it is reasonable to hypothesize that ADC is transcriptionally regulated during morphogenesis and may eventually be posttranslationally regulated in response to stress.

In hop, wounding of internodes and culture conditions leading to organogenic nodule formation led to accumulation 24 hours after culture initiation of the 24 kD band, whereas the 54

kD band remained constant at this stage. This result suggests that the 24 kD polypeptide may be important in response to an abiotic stress such as wounding or osmotic pressure due to culture medium composition. The product of ADC, putrescine, also increased already 24 hours upon internodes inoculation. ADC activity has been linked to stress responses.^{2,9} It is known that PAs are capable of protecting membranes against ROS-induced lipid peroxidation.¹⁵ The increase in PAs content at an early stage as detected in this work may be also related to an anti-oxidant role that has been attributed to PAs.

Arginine decarboxylase and ornithine decarboxylase genes were expressed in apple cells and stressed shoots.³⁸ According to these authors ADC expression correlates with cell growth and stress responses to chilling, salt and dehydration, suggesting that ADC is a primary biosynthetic pathway for putrescine biosynthesis in apple.

It has been demonstrated in various plant tissues that ODC pathway is particularly active in cell proliferation and that the ADC pathway is involved in embryo and organ differentiation and stress responses.²⁴

Recently, metabolic profiling during morphogenesis in hop showed a significant decrease in arginine levels in induced cultivated internodes and organogenic nodules,²³ suggesting that this amino acid may be channeled for PA synthesis through ADC activity.

Levels of ADC protein, corresponding to both 54 kD and 24 kD polypeptides, kept increasing during the morphogenic stages of prenodules and nodules suggesting the role of ADC and its product on morphogenesis. The fact that the 24 kD band is not detected 45 days after culture initiation and the 54 kD band decreased at this stage may suggest a feed-back regulation of de novo synthesis of ADC. Immunogold labeling also detected ADC after 45 days although at a low extent (data not shown). Since putrescine levels also decreased drastically it may be that putrescine is oxidized and serve as a source of H₂O₂ or alternatively may form conjugates as suggested by an increased ratio of conjugated versus total PAs 45 days after culture initiation.

During plantlet regeneration from organogenic nodules (after 45 days) the ratio conjugated/total PAs increases 2.95- and 1.18-fold comparing to 15 and 28 days of culture, respectively. This increase is mainly due to the increase in conjugated spermidine. Conjugated amines accumulate dramatically in response to certain developmental or stress factors.^{8,39}

Polyamine conjugation seems to be advantageous for the long-term regulation of free PA levels. This mechanism allows to reduce the risk of accumulation of harmful metabolites, produced by oxidative deamination.³⁹ Jasmonates have been shown to induce over-accumulation of methylputrescine and conjugated PAs in *Hyoscyamus muticus* L. root cultures.⁴⁰ Jasmonic acid and its precursor 12-oxophytodienoic acid increased in hop nodules after 45 days of culture.⁴¹ This increase in jasmonic acid may thus influence the relative accumulation of conjugated PAs

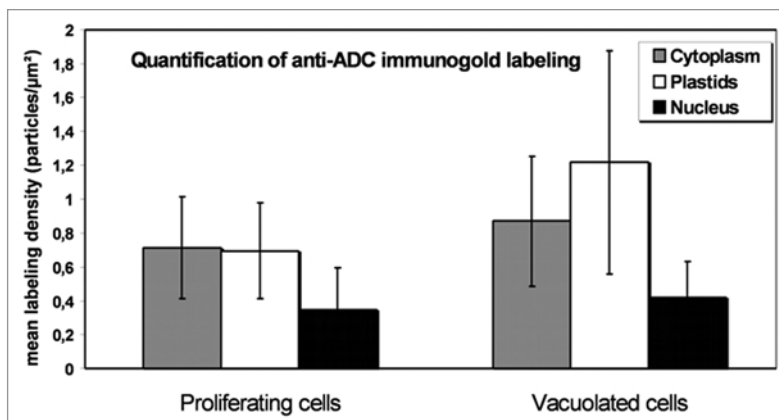


Figure 5. Histogram representing labeling density in different cellular compartments of nodular cells following anti-ADC immunolocalization. In proliferating cells labeling density is similar in plastids and cytoplasm. Plastids showed the highest labeling density in vacuolated nodular cells.

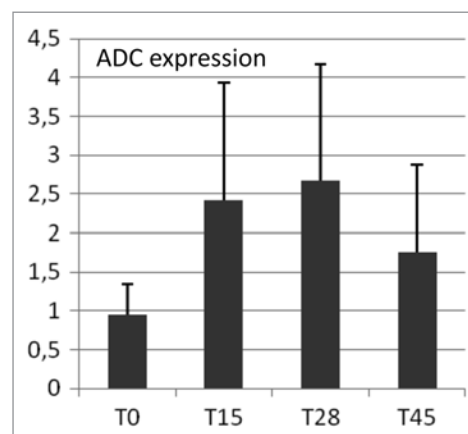


Figure 6. Quantitative RT-PCR analysis. Gene expression (ratio ADC vs. 18S) was studied at time of excision from parent plants (T0) and during organogenic nodule formation at 15, 28 and 45 days (T15, T28, T45) after culture initiation.

or may stimulate their oxidation through activation of DAO and PAO. Previously, it was shown an increase in lipid peroxides (precursors of jasmonates) during plantlet regeneration from organogenic nodules and related to an increase in reactive oxygen species content.^{21,22} An increase in DAO activity leads to generation of hydrogen peroxide.⁶ This compound may lead to subsequent triggering of programmed cell death. A programmed cell death may be taking place in tissues surrounding nodules, which may provide an extra source of carbon and nitrogen for the growing plantlets. In fact, H₂O₂ could be noticed in necrotic areas leading to nodule separation and mainly in surrounding *calli* tissues. Polyamines could play a role in the relocation or storage strategy of nitrogen together with their involvement in stress response.

Organized development in cultured tissues such as somatic embryogenesis is promoted by stress treatments, and may constitute a stress response.⁴² The arrangement of new cells into organized structures might depend on a genetically controlled balance

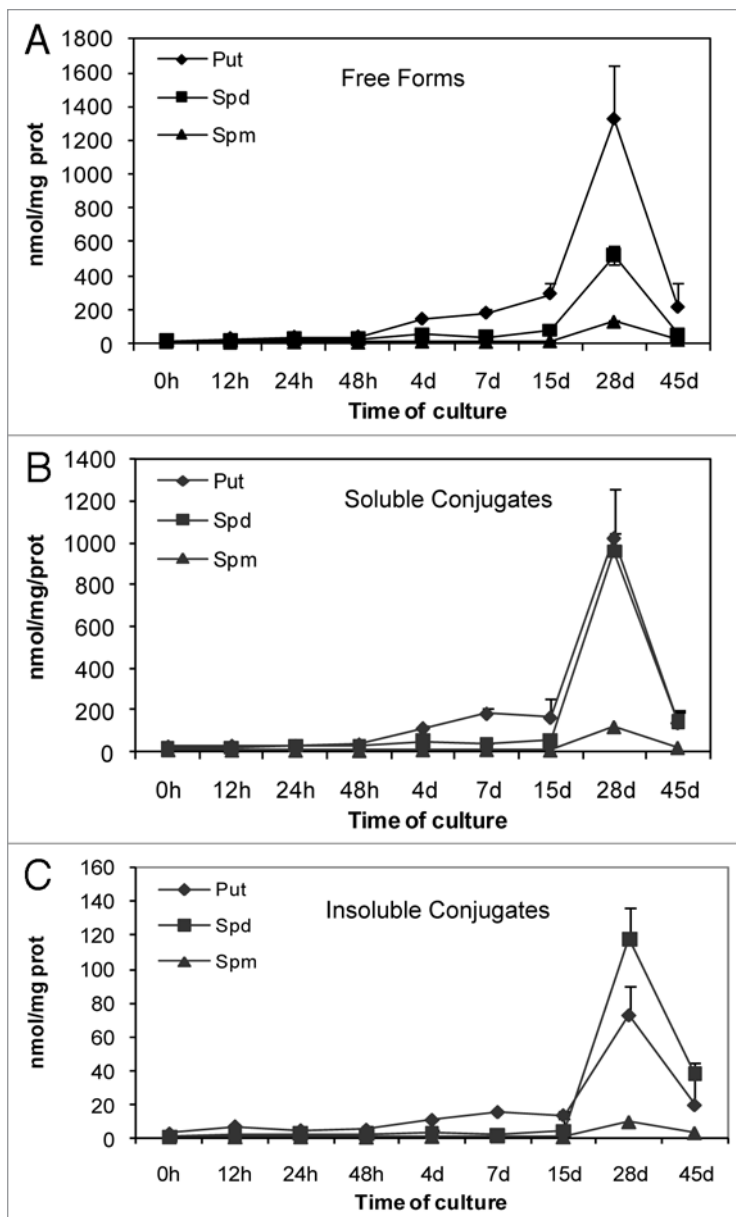


Figure 7. Changes in PAs levels (Put, Spd and Spm) during organogenic nodule formation and plantlet regeneration in hop. (A) Free forms. (B) TCA-soluble conjugates. (C) TCA-insoluble conjugates. Each value represents the mean of three independent experiments \pm SE.

between cell proliferation and cell death. In hop cultures, genes generally involved in stress response such as those coding for peroxidases and glutathione S-transferase are upregulated during the process of organogenic nodule formation.²³ Preliminary experiments showed that internodes treated with 10 mM N-acetyl-cysteine, an efficient antioxidant, never formed organogenic nodules. However, when 0.4 mM N-acetyl-cysteine was used no effect in nodule formation was observed (data not shown). These results suggest that there is a minimal threshold of ROS concentration for morphogenic processes to occur; although this topic deserves further research. The increase in ROS shown here may either constitute solely a physiological response to the

stress inherent to in vitro culture conditions which causes increased PA synthesis and PA catabolism or may also trigger this morphogenic process in hop.

Our data provide evidence that PAs are involved in organogenic nodule formation and they may contribute to an efficient response to stress as well as to a regulation of nutrient management, cell growth and differentiation occurring during this process of development.

Materials and Methods

Plant material and culture conditions. Internodes from *Humulus lupulus* (var. *Nugget*) plants, maintained under in vitro conditions, were induced to form organogenic nodules according to the protocol previously described in reference 20. Internodes of 6–9 mm long were wounded throughout by several incisions (3–5) using a razor blade (wounding treatment) before inoculation in MS medium.⁴³ Material was sampled at the following stages: (1) internodes at the time of excision from the parent plant (T0); (2) internodes grown for 12 h (T12 h), 24 h (T24 h) and 48 h (T48 h); (3) internodes grown for 4 days (T4d) showing divisions in cambial cells; (4) internodes grown for 7 days showing divisions in cambial and cortical cells (T7d); (5) internodes grown for 15 days on culture medium in which several prenodule structures are formed inside the calli (T15d); (6) nodule forming tissue after 28 days of culture (T28d); and (7) organogenic nodules regenerating plantlets after 45 days of culture (T45d).

Histochemical detection of ROS. Plant material from the different assay conditions and culture time-points was incubated under vacuum in sodium phosphate buffer 10 mM (pH 7.8) containing NBT 0.5% (w/v), NADPH 10 μ M and EDTA 10 μ M.⁴⁴ After remaining 15 minutes under light and at room temperature the samples were transferred to chloric hydrate solution (2.5 g/mL) and maintained at 4°C until observation under magnifying lenses (CETI) and photographed [Minolta (X-300 S) and Kodak film (100 ASA)].

Hydrogen peroxide was detected in plant material by incubation in DAB-HCl solution (1 mg/mL) (pH 3.8) (Sigma, MO; # D-8001) for 5–10 minutes in the dark, after which the material was transferred to ethanol 96% (v/v) and maintained at 4°C until observation. Control internodes with 15 days in culture were incubated in DAB-HCl solution supplemented with catalase 1,000 U/mL and treated as described above.

Extraction of proteins and immunoblot analysis. Proteins were extracted as previously described in reference 21, using an extraction buffer as reported by reference 34, and subjected to electrophoresis on a discontinuous gradient of SDS-polyacrylamide consisting of a 12% (w/v) acrylamide resolving gel and a 6% (w/v) stacking gel. Thirty μ g total protein was loaded per lane together with prestained standard proteins.

After electrophoresis, proteins were transferred to Immobilon membranes (Millipore) and an equal loading was confirmed by

Ponceau S staining. For the immunodetection, membranes were incubated for 2 h at room temperature with a rabbit polyclonal antibody raised against ADC from tobacco,³³ diluted 1:2,000 in the blocking buffer (2% powdered skimmed milk, 0.05% Tween-20 in PBS). After rinses in washing buffer, membranes were incubated for 2 h with alkaline phosphatase-conjugated anti-rabbit IgG (Boehringer Mannheim), diluted 1:1,000 in the blocking buffer. Finally, the proteins recognized by the antibody were revealed by treatment with a NBT-BCIP mixture. Controls were made, by replacing the first antibody with pre-immune serum.

Immunocytochemistry and quantification of immunogold labeling. Samples were fixed overnight at 4°C in 4% (w/v) paraformaldehyde in phosphate buffered saline (PBS). After three PBS washes (5 min each), samples were dehydrated in a methanol series at 4°C, washed in pure methanol, infiltrated and embedded in Lowicryl K4M at -30°C and finally polymerized under UV irradiation. Semithin (2 μm-thick) sections were obtained for preliminary histological analysis. For immunogold labeling, Lowicryl ultrathin (~100 nm) sections were collected on formvar- and carbon-coated nickel grids. Immunogold labeling was performed essentially as previously described in reference 45 and 46. Grids carrying Lowicryl ultrathin sections were sequentially floated on drops of double-distilled water and PBS for few minutes, and 5% BSA (bovine serum albumin) in PBS for 5 minutes. Then, grids were incubated for 1 h at room temperature with the same anti-ADC antibody used for the immunoblot analyses, diluted 1:10 in 1% BSA in PBS. After three washes in PBS containing 1% BSA, sections were incubated with a goat anti-rabbit IgG conjugated to 10 nm colloidal gold (BioCell), diluted 1:25 in 1% BSA in PBS for 45 min. Finally, grids were washed, air-dried, counterstained with 5% aqueous uranyl acetate and lead citrate, and observed in a Philips CM10 transmission electron microscope operating at 100 kV. Two different controls were performed in parallel, either by excluding the anti-ADC antibody or substituting it by preimmune serum. Quantification of immunogold labeling was designed as previously described in reference 45. Sampling was carried out over a number of micrographs randomly taken from different cells (corresponding to 28 days of culture) on each grid. The number of micrographs was determined using the progressive mean test,⁴⁷ with a minimum confidence limit of 0.05. Labeling density was defined as the number of particles per area unit (μm²). This number of particles was determined by hand counting particles over the compartments under study (cytoplasm, nucleus and plastids). Estimation of background was performed over cell walls, vacuoles, starch deposits and resin. The area in μm² was measured using a square lattice composed of 11 x 16 squares of 15 x 15 mm each. For each cell type and subcellular compartment, labeling density was expressed as mean labeling density of all micrographs ±SD and statistically compared using a Student's t-test, with α ≤ 0.05.

RNA extraction, cloning of ADC and quantitative RT-PCR. Total RNA was isolated essentially as described by reference 46. To further purify RNA, DNase treatment was carried out according to suppliers' instructions (Invitrogen). Samples were then extracted in phenol/chloroform/isoamylalcohol (75:24:1,

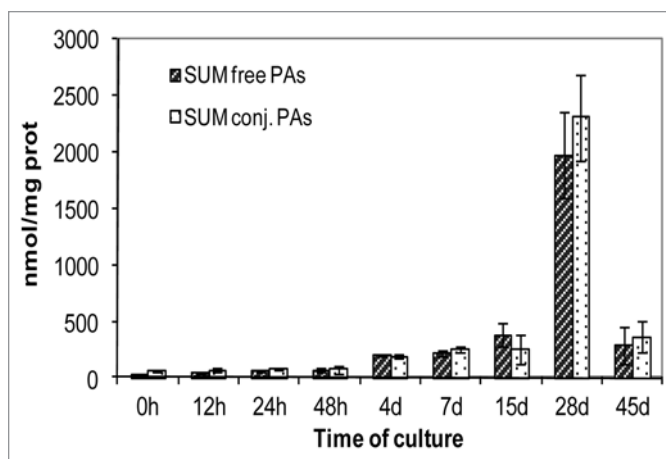


Figure 8. Total amount of free and conjugated PAs during organogenic nodule formation and plantlet regeneration in hop. Each value represents the mean of three independent experiments ±SE.

v/v/v), precipitated with sodium acetate and ethanol, washed in 70% ethanol and dissolved in water.

For cloning of ADC a reverse transcriptase-PCR based cloning approach was used. Degenerated primers were designed through alignment of known sequences available at GenBank: AF045669, AY337607, AF045667, Z37540, AJ871577, BT000682, AY491513, AF045686, X96791, AY274822, AF045683, AB110952 and AF045674. A touch-down PCR protocol with annealing for 20 cycles at 65°C and 20 cycles at 55°C, using AccuPrime™ Pfx DNA Polymerase (Invitrogen, Cat. No. 12344-024) was performed for the amplification of a hop ADC with the primers ADC-U205 (5'-GAY GGA TGG GGH GCT CCB TAT TTC-3') and ADC-L1931 (5'-AAC ATB AKY TCV GGC TCR TGC TGC AT-3'). The amplicons were cloned using the pGEM cloning kit (Promega, Cat. No. A1360) with a first step A-tailing procedure according to manufacturer's instructions.

Three-five μg of total RNA for each biological replicate was used to synthesize cDNA separately. Complementary DNAs were then quantified using Nanodrop. qPCR reactions were performed with the 7300 Real Time PCR System (Applied Biosystems) using Maxima™ SYBR Green qPCR Master Mix (Fermentas, Cat. No. K0221) on a Superplate 96-well PCR plate (ABgene, Thermo Scientific, Cat. No. AB-0600) according to the manufacturer's instructions. Amplicons were generated during 45 cycles with annealing temperature set at 55°C. The following primers were used: HIADCF (5'-TTC GGG TTT CGC AGA GTG AC-3') and HIADCR (5'-CAT CAC TGC AGC ATG GAC CT-3') for amplification of a 75 bp amplicon. Relative expression was calculated using the *Humulus lupulus* 18S ribosomal RNA gene for normalization. Negative control reactions without template were always included. Two-three biological replicates and two technical replicate were performed per time point. The means from 4–5 qRT-PCR reactions are presented for each time point.

Quantification of polyamines. Plant material was extracted in 5% (w/v) TCA (600 mg plant material/mL TCA). The

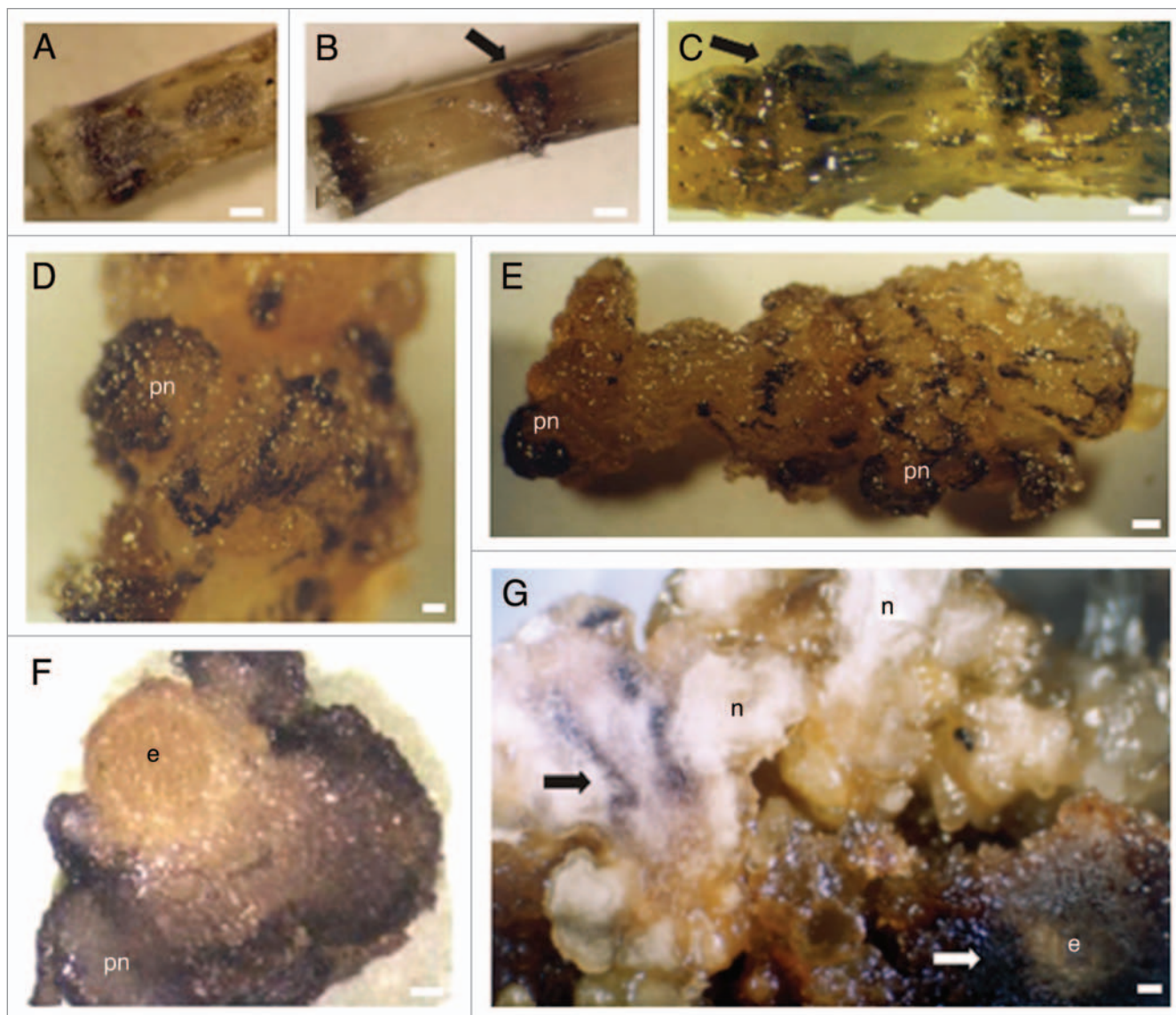


Figure 9. Tissue specific distribution of ROS following staining with NBT (A–E and G) and DAB (F). (A) Internode at the time of excision from the parent plant. Dark purple spots identifying ROS are seen. (B) Internode 24 hours upon wounding showing intense NBT staining at the cutting regions. (C) Internode seven days upon wounding. *Calli* cells concentrated in previously wounded areas show intense NBT staining (arrow). (D) Aspect of a pre-nodule (pn) arising 15 days upon internodes inoculation showing cells stained dark purple. (E) Internode 15 days upon wounding showing pre-nodules with intense accumulation of ROS. (F) Internode section showing a pre-nodule stained with DAB. (G) Cluster of nodules (n) 45 days after internodes inoculation. Initial explant (e) has proliferated giving rise to *calli* cells which appeared intensively stained (white arrow). Bars in A–C and F = 0.6 cm. Bar in E = 0.3 cm. Bars in F and G = 0.5 cm.

homogenates were centrifuged for 20 min at 13,000 rpm. The bound amines in the supernatant and the insoluble amines in the pellet (resuspended in the original volume of NaOH 1 M) were released by treating the fractions with 6 N HCl at 110°C for 18 h in a sealed ampule. After heating, the samples were centrifuged for 5 min at 13,000 rpm, dried under a stream of air at 80°C and resuspended in TCA. TCA extracts were analyzed for free, soluble and insoluble PAs following dansylation. The dansylation mixture consisted of 200 µL TCA extract (equivalent to about 20 mg fresh tissue), 400 µL dansyl chloride (5 mg/mL in acetone) and 200 µL saturated Na₂CO₃. After overnight incubation at room temperature the reaction was stopped

by addition of 100 µL proline (100 mg/mL). Dansylpolyamines were extracted in 0.5 mL of toluene by collecting the organic phase, drying and dissolving in 0.8 mL of acetonitrile. Finally the samples were filtered through a 0.45 µm filter. The standard sample was treated as described above and consisted of a mixture of 0.05 mM diaminopropane, putrescine, cadaverine, 1,7-diaminoheptane, spermidine and spermine. Aliquots were analyzed by reversed-phase HPLC⁴⁸ using the system HPLC (PHENOMEX). The dansylpolyamines injected in the column [Sphereclone 5 µm ODS (2), 250 x 4.60 m², ser#386140] were eluted in a gradient of acetonitrile and water of 70% (v/v) acetonitrile and 30% water for 5 min, 100% (v/v) acetonitrile for

4 min, 70% (v/v) acetonitrile and 30% water for 5 min, after which the initial conditions were re-established in the chromatography system (Applied Biosystems). Elution of the dansylpolyamines was performed at 25°C with a flow rate of 1.5 mL/min and monitored at 252 nm.

Note

The nucleotide sequence reported in this paper has been submitted to NCBI under accession number: ADC, Genbank Acc. GQ981435.

Acknowledgements

This work was partially supported by the Portuguese Foundation for Science and Technology (FCT) through a Post-Doc grant to

Ana M. Fortes (SFRH/BPD/27122/2006) and project ERA-PG/0004/2006-GRASP and COST Action FA0605 (Signaling control of stress tolerance and production of stress protective compounds in plants). The authors would like to thank Dr. Alexandra Cordeiro for the extremely valuable help provided for polyamine analyses. A.F.T. acknowledges grants from “Ministerio de Educación y Ciencia”, Spain (BIO2005-09252-C02-01 and BIO2008-05493-C02-01) and COST Action FA0605. K.P. acknowledges financial support from SFB 592, the Excellence Initiative of the German Federal and State Governments (EXC 294, EU FP6, DLR, ESA and Bundesministerium für Bildung und Forschung-BMBF).

References

- Tiburcio A, Altabella T, Borrell A, Masgrau C. Polyamine metabolism and its regulation. *Physiol Plant* 1997; 100:664-74.
- Alcázar R, Marco F, Cuevas J, Patron M, Ferrando A, Carrasco P, et al. Involvement of polyamines in plant response to abiotic stress. *Biotechnol Lett* 2006; 28:1867-76.
- Vuosku J, Jokela A, Läärä E, Sääskilähti M, Muilu R, Sutela S, et al. Consistency of polyamine profiles and expression of arginine decarboxylase in mitosis during zygotic embryogenesis of Scots pine. *Plant Physiol* 2006; 142:1027-38.
- Thomas T, Thomas T. Polyamines in cell growth and cell death: molecular mechanisms and therapeutic applications. *Cell Mol Life Sci* 2001; 58:244-58.
- Kusano T, Berberich T, Tateda C, Takahashi Y. Polyamines: essential factors for growth and survival. *Planta* 2008; 228:367-81.
- Cona A, Rea G, Angelini R, Federico R, Tavliadoraki P. Functions of amine oxidases in plant development and defence. *Trends Plant Sci* 2006; 11:80-8.
- Liu J, Nada K, Honda C, Kitashiba H, Wen X, Pang X, et al. Polyamine biosynthesis of apple callus under salt stress: importance of the arginine decarboxylase pathway in stress response. *J Exp Bot* 2006; 57:2589-99.
- Scoccianti V, Sgarbi E, Fraternali D, Biondi S. Organogenesis from *Solanum melongena* L.-(eggplant) cotyledon explants is associated with hormone-modulated enhancement of polyamine biosynthesis and conjugation. *Protoplasma* 2000; 211:51-63.
- Bouchereau A, Aziz A, Larher F, Martin-Tanguy J. Polyamines and environmental challenges: recent development. *Plant Sci* 1999; 140:103-25.
- Groppa M, Benavides M. Polyamines and abiotic stress: recent advances. *Amino Acids* 2008; 34:35-45.
- Pandey S, Ranade S, Nagar P, Kumar N. Role of polyamines and ethylene as modulators of plant senescence. *J Biosci* 2000; 25:291-9.
- Tun N, Santa-Catarina C, Begum T, Silveira V, Handro W, Floh E, et al. Polyamines induce rapid biosynthesis of nitric oxide (NO) in *Arabidopsis thaliana* seedlings. *Plant Cell Physiol* 2006; 47:346-54.
- Kuehn G, Phillips G. Role of polyamines in apoptosis and other recent advances in plant polyamines. *Crit Rev Plant Sci* 2005; 24:123-30.
- Moschou P, Sarris P, Skandalis N, Andriopoulou A, Paschalidis K, Panopoulos N, et al. Engineered polyamine catabolism preinduces tolerance of tobacco to bacteria and oomycetes. *Plant Physiol* 2009; 149:1970-81.
- Tadolini B, Hakim G. Interaction of polyamines with phospholipids: spermine and Ca²⁺ competition for phosphatidylserine containing liposomes. *Adv Exp Med Biol* 1988; 250:481-90.
- Papadakis A, Roubelakis-Angelakis K. Polyamines inhibit NADPH oxidase-mediated superoxide generation and putrescine prevents programmed cell death induced by polyamine oxidase-generated hydrogen peroxide. *Planta* 2005; 220:826-37.
- McCown B, Zeldin E, Pinkalla H, Dedolph R. Nodule culture: a developmental pathway with high potential for regeneration, automated micropropagation and plant metabolite production from woody plants. In: Hanover J, Keathley D, Eds. Genetic manipulation of woody plants. New York: Plenum 1988;149-66.
- Van Cleemput M, Cattoor K, De Bosscher K, Haegeman G, De Keuleire D, Heyerick A. Hop (*Humulus lupulus*)-derived bitter acids as multipotent bioactive compounds. *J Nat Prod* 2009; 72:1220-30.
- Fortes A, Santos F, Pais M. Organogenic nodule formation in hop: a tool to study morphogenesis in plants with biotechnological and medicinal applications. *J Biomed Biotechnol* 2010; 2010.
- Fortes A, Pais M. Organogenesis from internode-derived nodules of *Humulus lupulus* var. *Nugget* (Cannabaceae): histological studies and changes in the starch content. *Am J Bot* 2000; 87:971-9.
- Fortes A, Coronado M, Testillano P, Risueño MC, Pais M. Expression of lipoxigenase during organogenic nodule formation from hop internodes. *J Histochem Cytochem* 2004; 52:227-41.
- Silva M, Fortes A, Testillano P, Risueno M, Pais M. Differential expression and cellular localization of ERKs during organogenic nodule formation from internodes of *Humulus lupulus* var. *Nugget* Eur J Cell Biol 2004; 83:425-33.
- Fortes A, Santos F, Choi Y, Silva M, Figueiredo A, Sousa L, et al. Organogenic nodule development in hop (*Humulus lupulus* L.): transcript and metabolic responses. *BMC Genomics* 2008; 9:445.
- Gemperlová L, Eder J, Cvikrová M. Polyamine metabolism during the growth cycle of tobacco BY-2 cells. *Plant Physiol Biochem* 2005; 43:375-81.
- Jubault M, Hamon C, Grivot A, Lariagon C, Delourme R, Bouchereau A, et al. Differential regulation of root arginine catabolism and polyamine metabolism in clubroot-susceptible and partially resistant *Arabidopsis* genotypes. *Plant Physiol* 2008; 146:2008-19.
- Papadakis A, Paschalidis K, Roubelakis-Angelakis K. Biosynthesis profile and endogenous titers of polyamines differ in totipotent and recalcitrant plant protoplasts. *Physiol Plant* 2005; 125:10-20.
- Bachrach U, Wang Y, Tabib A. Polyamines: new cues in cellular signal transduction. *News Physiol Sci* 2001; 16:106-9.
- Bertoldi D, Tassoni A, Martinelli L, Bagni N. Polyamines and somatic embryogenesis in two *Vitis vinifera* cultivars. *Physiol Plant* 2004; 120:657-66.
- Pedroso M, Primikiriou N, Roubelakis-Angelakis K, Pais M. Free and conjugated polyamines in embryonic and non embryonic leaf regions of camellia leaves before and during direct somatic embryogenesis. *Physiol Plant* 1997; 101:213-9.
- Gemperlová L, Fischerová L, Cvikrová M, Malá J, Vondráková Z, Martincová O, et al. Polyamine profiles and biosynthesis in somatic embryo development and comparison of germinating somatic and zygotic embryos of Norway spruce. *Tree Physiol* 2009; 29:1287-98.
- Clay N, Nelson T. *Arabidopsis* thickvein mutation affects vein thickness and organ vascularization and resides in a provascular cell-specific spermine synthase involved in vein definition and in polar auxin transport. *Plant Physiol* 2005; 138:767-77.
- Santos F. Studies of polar auxin transport in *Humulus lupulus* morphogenic process and isolation of proteins interacting with PIN1- a putative auxin efflux carrier of *Arabidopsis thaliana*. Ph.D., thesis Science Faculty of Lisbon: University of Lisbon 2006.
- Bortolotti C, Cordeiro A, Alcázar R, Borrell A, Culiñez-Macia F, Tiburcio A, et al. Localization of arginine decarboxylase in tobacco plants. *Physiol Plant* 2004; 120:84-92.
- Borrell A, Culiñez-Macia F, Altabella T, Besford R, Flores D, Tiburcio A. Arginine decarboxylase is localized in chloroplasts. *Plant Physiol* 1995; 109:771-6.
- Malmberg R, Smith K, Bell E, Cellino M. Arginine decarboxylase of oats is clipped from a precursor into two polypeptides found in the soluble enzyme. *Plant Physiol* 1992; 100:146-52.
- Schipper R, Romain N, Otten A, Tan J, Lange W, Verhofstad A. Immunocytochemical detection of ornithine decarboxylase. *J Histochem Cytochem* 1999; 47:1395-404.
- Beigbeder A, Vavadias M, Navakoudis E, Kotzabasis K. Influence of polyamine inhibitors on light-independent and light-dependent chlorophyll biosynthesis and on the photosynthetic rate. *J Photochem Photobiol B-Biology* 1995; 28:235-42.
- Hao Y, Kitashiba H, Honda C, Nada K, Moriguchi T. Expression of arginine decarboxylase and ornithine decarboxylase genes in apple cells and stressed shoots. *J Exp Bot* 2005; 56:1105-15.
- Cvikrova M, Mala J, Hrubcova M, Eder J, Zon J, Machackova I. Effect of inhibition of biosynthesis of phenylpropanoids on sessile oak somatic embryogenesis. *Plant Physiol Biochem* 2003; 41:251-9.
- Biondi S, Fornalé S, Oksman-Caldentey KM, Eeva M, Agostani S, Bagni N. Jasmonates induce over-accumulation of methyl putrescine and conjugated polyamines in *Hyoscyamus muticus* L. root cultures. *Plant Cell Reports* 2000; 19:691-7.
- Fortes A, Miersch O, Lange P, Malhó R, Testillano P, Risueño MC, et al. Expression of allene oxide cyclase and accumulation of jasmonates during organogenic nodule formation from hop (*Humulus lupulus* var. *Nugget*) internodes. *Plant Cell Physiol* 2005; 46:1713-23.
- Thibaud-Nissen F, Shealy R, Khanna A, Vodkin L. Clustering of microarray data reveals transcript patterns associated with somatic embryogenesis in soybean. *Plant Physiol* 2003; 132:118-36.
- Murashige T, Skoog F. A revised medium for rapid growth and bioassays with tobacco tissue cultures. *Physiologia Plantarum* 1962; 15:473-97.

-
44. Doke N, Ohashi Y. Involvement of an o-2-generating system in the induction of necrotic lesions on tobacco-leaves infected with tobacco mosaic-virus. *Physiol Mol Plant Pathol* 1988; 32:163-75.
 45. Seguí-Simarro J, Austin Jn, White E, Staehelin L. Electron tomographic analysis of somatic cell plate formation in meristematic cells of *Arabidopsis* preserved by high-pressure freezing. *Plant Cell* 2004; 16:836-56.
 46. Rerie W, Whitecross M, Higgins T. Developmental and environmental regulation of pea legumin genes in transgenic tobacco. *Mol Gen Genet* 1991; 225:148-57.
 47. Seguí-Simarro J, Staehelin L. Cell cycle-dependent changes in Golgi stacks, vacuoles, clathrin-coated vesicles and multivesicular bodies in meristematic cells of *Arabidopsis thaliana*: a quantitative and spatial analysis. *Planta* 2006; 223:223-36.
 48. Marcé M, Brown D, Capell T, Figueras X, Tiburcio A. Rapid high-performance liquid chromatographic method for the quantitation of polyamines as their dansyl derivatives: application to plant and animal tissues. *J Chromatogr B Biomed Appl* 1995; 666:329-35.